

Package Reliability of MEMS Sensors Used in Automotive Under Random Vibration

Yue Liu^a, Bo Sun^{*}, Qiang Feng

School of reliability and systems engineering, Beihang University, Beijing 100191, China
sunbo@buaa.edu.cn

The package and interconnection are critical concerns that influence the reliability of MEMS sensors applied in modern automotive under random vibration conditions. This paper conducts a research on this problem to reveal the reliability and influencing factors of MEMS on board level using finite element modelling and random vibration response simulation method. The ADXL78 MEMS chip is used as an example. Model analysis has been used to obtain the frequency character of MEME sensor. The loading is power spectral density of different pavement levels obtained from Belgium pavement test in GB/T 7031-2005 (Mechanical vibration-road pavement spectrum measurement data report). Random Vibration analysis has been used to obtain the solder joint maximum equivalent stress of ADXL78. The results show that the MEMS package solder joint is the weakness point in the structure to fatigue failure. The engineering design and application suggestions for improving the packaging reliability of MEMS are presented through the sensitive factors analysis.

1. Introduction

Micro-Electro-Mechanical Systems (MEMS) have many advantages, such as small size, light weight, low energy consumption, small inertia, and short response time (Krueger, 2001 and Bradford, 2004). Nowadays, as a result of the fast development of global electronization and intellectualization, MEMS sensors become more widely used. In some high-end automobiles, the number of MEMS sensors may be hundreds or more. For example, BMW740i has more than 70 MEMS sensors (Eloy, 2002 and Grace, 2002).

During manufacturing, transporting and service, electronic components are subject to various kinds of vibration loadings. Particularly, vehicle-mounted conditions, in which electronic products experience a great amount of random vibration loadings during the whole service lifetime, make the vibration-induced failure one of the most important reliability issues. For example, the value will go up to 2.5g when the automobile drives on the dirt road. On this occasion, the typical failure mechanism of MEMS sensors consists of adhesion, particle pollution, hierarchy, fatigue, corrosion and fracture (Hsu, 2006). Especially, the fatigue failure of MEMS sensors caused by vibration and thermal cycle is the major failure mode.

Focused on the failure mode and reliability of MEMS sensors, many studies have been reported in the literature. Mariani (2009) characterized the properties of polysilicon MEMS and presented the association between the morphology of polysilicon film constituting the movable parts of the sensor and MEMS failure. Jamborhazi (2010) detected and predicted the failure of MEMS by monitoring the resonant frequency. Other researchers focused on the reliability of MEMS sensors under different environments (such as temperature, humidity, vibration, shock, and stress of automotive electronic units). For example, David (2007) focuses on the thermo-mechanical analysis of a commercial LFBGA package.

At the same time, the issues of the failure and reliability of package and interconnection of electronic products under random vibration had been discussed. Some researchers presented the reliability and fatigue failure of solder joints in different packaging, like FBGA (Fine-Pitch Ball Grid Array) (Eckert, 2009), BGA (Ball Grid Array) (Da, 2010), PBGA (Plastic Ball Grid Array) (Wang, 2004) and FCBGA (Flip-chip Ball Grid Array) (Pustan, 2007), under thermal or vibration conditions.

All in all, there have been some researches focused on the failure mode and reliability of internal structure and interconnection of MEMS under different environments. In contrast to the previous research, there is little study about LCC (Leadless Chip Carrier) which is one typical package of MEMS. The authors' team once conducted a research to reveal the influencing factors and assess package reliability of LCC package under the impact loadings (Cui, 2011).

In this paper, a MEMS sensor ADXL78 has been used for reliability analysis. Finite element modelling and random vibration analysis are used. Sensitivity analysis has been conducted by changing the main parameters to study these factors on the influence of the package and interconnection reliability.

2. Case description

2.1 Device information

An ADXL78 MEMS sensor made by Analog Devices Inc. in USA is used for study. ADXL78 is a low power, complete single-axis accelerometer with signal conditioned voltage outputs that are on a single monolithic IC. This product measures acceleration with a full-scale range of ± 35 g, ± 50 g, or ± 70 g (minimum). It can also measure both dynamic acceleration (vibration) and static acceleration (gravity). The ADXL78 is temperature stable and accurate over the automotive temperature range, with a self-test feature that fully exercises all the mechanical and electrical elements of the sensor with a digital signal applied to a single pin (ADI, 2013).

ADXL78 board level encapsulation structure consists of alloy cover, ceramic body, PCB board, and solder joints. The detailed structure parameters (unit: mm) are shown in Figure 1. The important component structure is installed in the ceramic packaging body and is covered using brazing technology in the vacuum. Due to its relative less mass compared with the external structure and the less-focused subject in our analysis, a simplified process is applied in this paper.

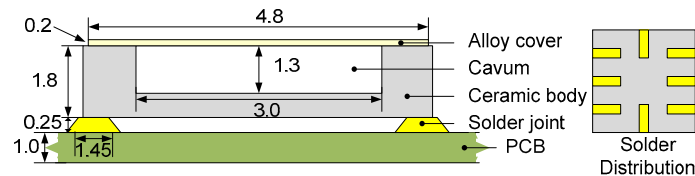


Figure 1: MEMS structure parameters

2.2 Loading information

Different pavements may give rise to two kinds of vibration excitation. One is discrete event excitation, such as the bow pavement and undulate pavement. Another is random pavement vibration excitation, such as various grades of the highway pavements. The vibration excitation is different as the automobiles driving on different grades of pavements.

The simulation for the pavement toughness can be classified into two kinds of methods. One is combined given pavement power spectral density (PSD) and the vibration properties of the system to calculate the output power spectral density of relevant parameter using random vibration theory. Another method is to transform the given pavement power spectral density into time signal by fast Fourier transform (FFT), and then import it into the system to gain the relevant PSD (Tan, 2000). Random vibration excitation is used in this paper and the first simulation method is chosen to transform this excitation. The time signal from pavement vibration real-time monitoring is transformed to pavement power spectral density through FFT.

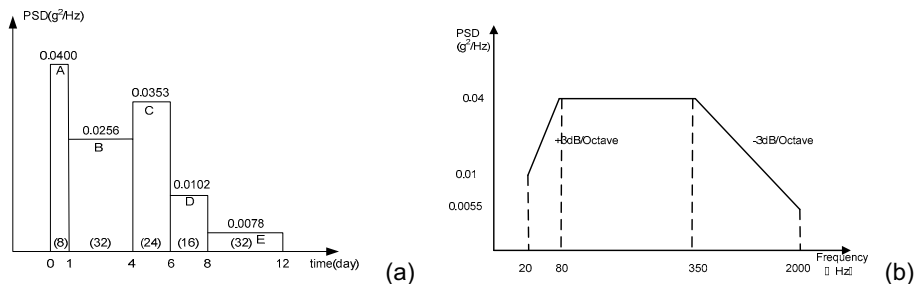


Figure 2: PSD and velocity of different pavement levels

In order to get different PSD of pavement levels, this paper refers to the pavement spectral test and data developed in Xstad Belgium (GB7031, 2005). In this test, there are five pavement levels. It keeps uniform driving over the whole experiments, and there is no obvious braking. The PSD data of different pavement levels is shown in Figure 2 (a). The PSD of the A level is presented in Figure 2 (b). The abscissa is the running time at each level, for example, at A level the car runs one day and at B level the car runs three days. The ordinate is the PSD. The velocities at each level are shown in the brackets. A level is a rough washboard road with 150 mm wave ridge every 2 m. B level is rocks road. C level is a kind of washboard road like rays with 50 mm to 100 mm wave ridge. D level is a kind of washboard road with 500 mm wave ridge. E level is a kind of road with small waves every 75 mm (GJB150, 2009).

3. Finite element analysis

3.1 Finite element model

A finite element model of ADXL78 is developed using ANSYA 13.0 commercial software. The element type of PCB is chosen as SHELL 95, while others are SOLID 185 3D. Table 1 shows the components material properties. The damping ratio is usually between 0.01 and 0.25. In this paper, 0.03 is chosen according to (Zhao, 2004). As the main object for analysis, solder interconnects at the critical locations are meshing in refinement. Finally, there are 9847 nodes and 6621 elements.

Table 1: MEMS components material properties

| Components | Density | Modulus of Elasticity | Poisson`s ratio |
|-------------------|----------|-----------------------|-----------------|
| Units | kg/m^3 | GPa | |
| PCB (FR4) | 1900 | 22 | 0.3 |
| Cover | 8460 | 138 | 0.31 |
| Body (ceramic) | 3920 | 344 | 0.22 |
| Solder (90Pb10Sn) | 8200 | 43 | 0.36 |

The PCB is bonded by four screws. As the boundary conditions, all nodes at the screw holes are fixed at all degrees of freedom. A 3D finite element model of ADXL78 is shown in Figure 3.

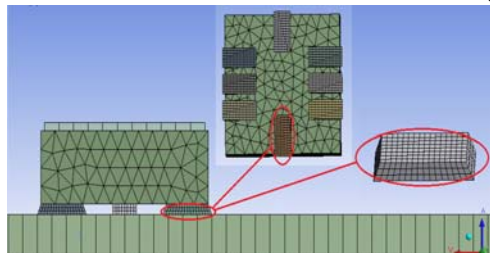


Figure 3: Finite element model of ADXL78

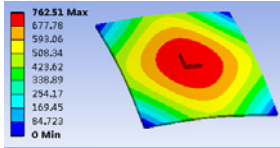
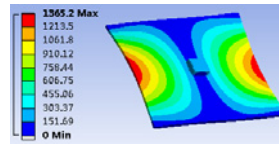
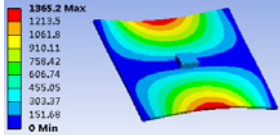
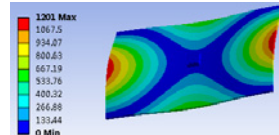
3.2 Modal analysis

Modal analysis aims at confirming the MEMS sensors properties, natural frequencies and mode shapes, which are very important parameters and provide an insight into the dynamics of system. Since the range of the vibration frequency in the case is 20Hz to 2000Hz, the range for analysis is set to be 10 Hz to 2500 Hz. The results are list in Table 2.

In the vibration reliability analysis procedure, one should not only ensure that the device has a higher natural frequency to avoid resonance, but also find out the weak links of the system. According to Table 2, in the 1st mode shape, there is a great deformation in the middle of the board. A great lateral deformation occurs in the last three mode shape.

PCB can produce large flexural deformation due to bending moment in high vibration. Large flexural deformation also generates on MEMS sensor. Relative displacement generates due to the different flexural deformations as the boundary conditions, structures, and materials of PCB and MEMS are different. When MEMS sensor is attached to the PCB with surface mounted arrangement, the relative displacement between the PCB and MEMS can generate a significant amount of strain in the solder joint. With the continuous vibration loading, changes of the strain in the solder joints make solder joints the weakest point in the structure.

Table 2: MEMS natural frequencies and mode shapes

| Mode | Natural Frequencies (Hz) | Mode shapes | Mode | Natural Frequencies (Hz) | Mode shapes |
|------|--------------------------|---|------|--------------------------|---|
| 1 | 378.85 |  | 3 | 1156.2 |  |
| 2 | 897.5 |  | 4 | 1635.4 |  |

3.3 Random vibration analysis

Random vibration analysis follows after harmonic analysis. The random vibration excitation is imported on the boundary of the LCC packaging. In other words, the PSD is imported on the four screw holes to calculate the maximum equivalent stress of the solder joints. The inputs are the power spectral density at each level shown in Figure 2.

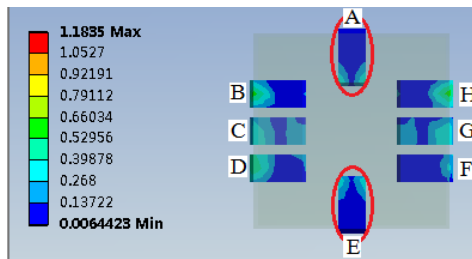


Figure 4: Random vibration analysis results (unit: MPa)

The equivalent stress, known as the Von Mises stress, is more appropriate to be used in the S-N curve to predict the fatigue life. The corner solder bodies A and E are observed to have stress concentration along the solder interface. The maximum equivalent stress of the solder joint is calculated as 1.18, which is shown in Figure 4. While the equivalent stress of solder joint B is 0.68 which is 74.4 % less than A. The equivalent stress of solder joint C is 0.41 which is 186 % less than A. The reliability distribution can be seen according to the stress data.

4. Design parameter sensitivity analysis

Solder joints are main weak links of LCC packaging devices and prone to fatigue failure under random vibration load. In packaging structure design and production process, many factors affect the reliability of the MEMS, such as welding, solder joint internal quality, solder joints shape, solder type, solder material mechanics characteristics, packaging type and size, device position on the PCB, PCB substrate size, PCB material characteristics, vibration load form, Poisson's ratio (Cui, 2011). This paper mainly analyzes the main influence factors in MEMS device design and process: the solder material, solder joint geometrical parameters, PCB substrate geometrical parameters. Considering the corresponding relations between the stress and the reliability, the maximum equivalent stress amplitude values are used to analysis how factors influences the MEMS device reliability by contrasting the solder joints under different conditions.

4.1 Solder material

In above analysis, Sn4.0Ag0.5Cu is used as solder material. Besides, Sn3.5Ag, Sn37Pb, Sn3.8Ag0.7Cu are also commonly used. Their material parameters show in the table 3 .Simulation analyses about these materials are conducted to calculate the maximum equivalent stress amplitude of the solder joints..

For different solder materials, the maximum equivalent stress of MEMS device packaging structure is still focused on the spot. Figure 5 (a) shows the maximum equivalent stress contrast diagram for different solder materials. The equivalent stress of lead materials is less than the other three kinds of lead-free materials, while in these three materials. The Sn3.8Ag0.7Cu has the lowest equivalent stress. To improve the device reliability, it is needed to reduce the maximum equivalent stress amplitude of packaging device

in the material design process. Considering the modern lead-free requirements, the Sn3.8Ag0.7Cu solder material is recommended.

Table 3: Different solder material parameter

| Material | Density(kg/m ³) | Young Modulus(GPa) | Poisson ratio |
|--------------|-----------------------------|--------------------|---------------|
| Sn4.0Ag0.5Cu | 8200 | 43.00 | 0.36 |
| Sn3.8Ag0.7Cu | 7424 | 38.00 | 0.38 |
| Sn3.5Ag | 7400 | 52.70 | 0.40 |
| Sn3.7Pb | 8640 | 38.58 | 0.40 |

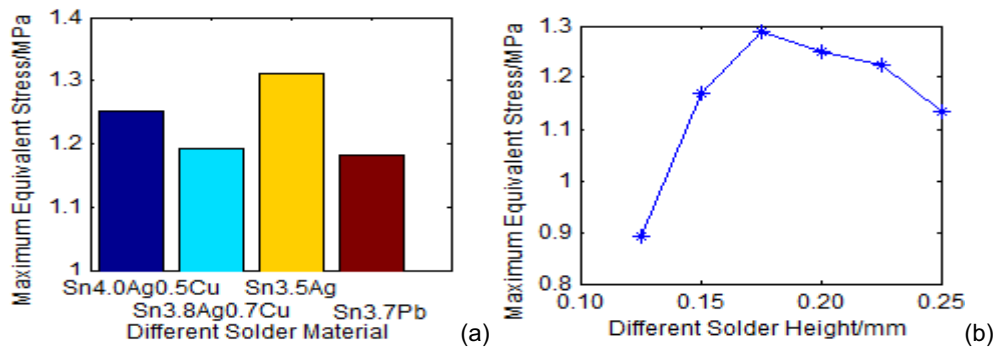


Figure 5: Maximum equivalent stress of different solder material and different solder height

4.2 Solder joint geometrical parameters

Among the solder joint technical parameters, the largest influence factor is the height of solder joints. In order to study the actual welding process affection on MEMS device reliability under random vibration conditions, this paper adjusts the solder joint height with other parameters steady. The maximum equivalent stress result is shown in Figure 5 (b).

Under random vibration conditions, with the increasing of the solder joints height, the maximum equivalent stress increases gradually at first and then reaches the maximum value 1.29 at 0.2mm height and trends to decrease. This phenomenon can be interpreted from two aspects. On the one hand, with the increase of the thickness, solder joint internal defects and empty holes will surely increase. The stress will concentrate on the defect place and empty hole, and this affects the mechanical properties of the solder joint, and reduces the reliability of solder joints. On the other hand, with the increase of the solder joints height, natural frequencies of the device increases beyond random vibration load frequency range, resonance phenomenon is abate. This makes the maximum equivalent stress amplitude of packaging decrease. With the technical limits, it is difficult to make the solder joint height less than 0.2 mm. While by increasing the solder joint height to reduce the maximum equivalent stress is easier. So it is suitable to enlarge the solder joint height to improve the reliability of the device.

4.3 PCB substrate geometrical parameters

In above analysis, the PCB substrate uses a rectangular base plate with the size of 40*50*1 (mm). To consider the influence of base plate size to components reliability, the base plate size and base plate thickness are changed. Different sizes of LCC package simulation analysis are conducted to calculate the equivalent stress of the solder joint. Results are shown in Figure 6.

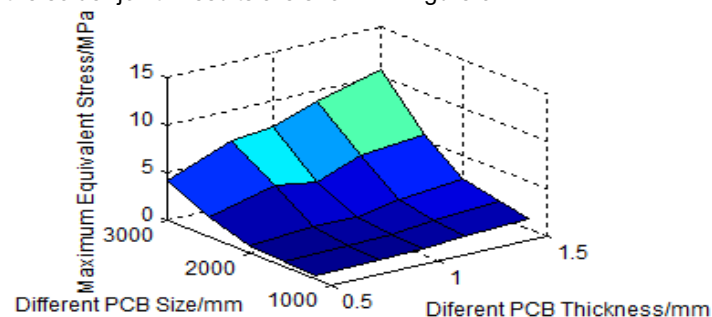


Figure 6: Maximum Equivalent Stress of Different PCB Substrate Geometric Parameters

With PCB substrate size or thickness reduction, the maximum equivalent stress value increases gradually. Compared with 30*40mm, the equivalent stress amplitude of 40*50mm increases 1.09 times, while compared with 40*50mm, 50*60mm's increases 4.74 times. It can be concluded that increasing PCB substrate size can achieve a rapid decline in the maximum equivalent stress. In order to achieve the purpose of reducing stress, it is suggested in the actual engineering increasing structure size and thickness within the allowable range.

5. Conclusion

This paper conducts key parameters sensitivity analysis to MEMS packaging design, process parameters, and gives the design and the application suggestion to improve the reliability of the MEMS packaging.

(1) Under the vibration situation, solder joints are the weak link of LCC packaging MEMS device. The maximum equivalent stress of packaging structure concentrates in the inside of the solder joint angle point, and at the same time, the base plate deforms under the action of stress.

(2) There are many factors influencing the fatigue life of solder vibration. It mainly consists of welding technique, solder joint internal quality, solder joints shape, solder type, welding material mechanics characteristics, packaging type and size, device position in the PCB, PCB board size, PCB material characteristics, vibration load form, and Poisson's ratio and so on.

(3) The maximum equivalent stress of the solder joints changes with different solder materials. With the increasing of the solder joints height, it increases first and then decreases. It decreases with the PCB base plate size and thickness decreasing. It is suggested conducting material simulation analysis increasing the solder joint height, and selecting size and thickness larger base plate to minimize stress.

References

- ADI (Analog Devices, Inc.), 2010, ADXL78 Accelerometers datasheet and product information <www.analog.com> accessed 20.01.2013
- Bradford S.D., Denison T., Kaung J., 2004, A Monolithic High-g SOI-MEMS Accelerometer for Measuring Projectile Launch and Flight Accelerations, Proc. Sensors, 296-299.
- Cui J.Z., Sun B., Feng Q., 2011, Finite Element Analysis of MEMS Package under High Impact, Journal of mechanical engineering, 47, 177 -185 (in Chinese).
- Da Y., Abdullah A.Y., Nguyen T., Seungbae P., Chung S., 2010, High-cycle Fatigue Life Prediction for Pb-free BGA under Random Vibration Loading, Microelectronics Reliability, 10, 1-8.
- Eckert T., Wolfgang H.M., Nilsson F.N., 2009, A Solder Joint Fatigue Life Model for Combined Vibration and Temperature Environments, Proc. Electronic Components and Technology Conference, 522- 528.
- Eloy J.C., Roussel P., Mounier E., 2002, Status of the Inertial MEMS-based Sensors in the Automotive, Yole Development France, 45, 43-48.
- GB T 7031, 2005, Mechanical vibration-road pavement spectrum measurement data report (in Chinese).
- GJB150.16A, 2009, Military equipment laboratory environment test method (in Chinese).
- Grace R., 2002, MEMS/MST Provide Updated Solutions Go Many Automotive Application: the Great Migration from Electromechanical and Discrete Approaches, MST News, 10, 12-14.
- Hsu T.R., 2006, Reliability in MEMS Packaging, Proc. 44th Reliability Physics Symposium, 398- 402.
- Jamborhazi S., Hegedus I., Rencz M., 2010, Simulating and Monitoring the Resonant Frequency of MEMS for Failure Detection and Prediction, Proc. 16th IEEE International Mixed-Signals, Sensors and Systems Test Workshop, 978-982.
- Krueger S., Grace R., 2001, New Challenges for Microsystems Technology in Automotive Applications, MST News, 1, 4-7.
- Mariani S., Ghisi A., Martini R., Corgliano A., Simoni B., 2009, A Multiscale-stochastic Finite Element Approach to Shock-induced Polysilicon MEMS Failure, Proc. 10th International Thermal, Mechanical and Multiphysics Simulation and Experiments in Micro-electronics and Micro-systems, 1-7.
- Pustan D., Fischer S., Wilde J., 2007, Analysis of Field Loads in Automotive ECUs and MEMS Sensors, Proc. Electronic Components and Technology Conference, 1696-1700.
- Tan R.H., Chen Y., Yao D.F., Lu Y.X., 2000, Automotive Vibration Simulation under Pavement Random Loading, Vibration, Test and Diagnosis, 20, 119-122.
- Wang H.F., Zhao M., Guo Q., 2004, Vibration Fatigue Experiments of SMT Solder Joint, Microelectronics Reliability, 44, 1143-1156.
- Zhao M., Zhou H.T., 2004, Mechanical vibration and noise. Science Press, Beijing, China (in Chinese).